

The submitted manuscript has been authored by a contractor of the U. S. Government under contract DE-AC05-84OR21400. Accordingly, the U. S. Government retains a nonexclusive, royalty free license to publish or reproduce the published form of this contribution, or allow others to do so, for U. S. Government purposes.

## ATF EDGE PLASMA TURBULENCE STUDIES USING A FAST RECIPROCATING LANGMUIR PROBE\*

T. UCKAN, C. HIDALGO\*\*, J.D. BELL, J.H. HARRIS, J.L. DUNLAP,  
G. R. DYER, P.K. MIODUSZEWSKI, J.B. WILGEN

*Oak Ridge National Laboratory, Oak Ridge, Tennessee 37831, U.S.A.*

Ch.P. RITZ, A.J. WOOTTON, T.L. RHODES, K. CARTER

*Fusion Research Center, The University of Texas, Austin, Texas 78712, U.S.A.*

Electrostatic turbulence on the edge of the Advanced Toroidal Facility (ATF) torsatron is investigated experimentally with a fast reciprocating Langmuir probe (FRLP) array. Initial measurements of plasma electron density  $n_e$  and temperature  $T_e$  and fluctuations in density ( $\bar{n}_e$ ) and plasma floating potential ( $\bar{\phi}_f$ ) are made in ECH plasmas at 1 T. At the last closed flux surface (LCFS,  $r/a \sim 1$ ),  $T_e \approx 20-40$  eV and  $n_e \approx 10^{12} \text{ cm}^{-3}$  for a line-averaged electron density  $\bar{n}_e = (3-6) \times 10^{12} \text{ cm}^{-3}$ . Relative fluctuation levels, as the FRLP is moved into core plasma where  $T_e > 20$  eV, are  $\bar{n}_e/n_e \approx 5\%$ , and  $e\bar{\phi}_f/T_e \approx 2\bar{n}_e/n_e$  about 2 cm inside the LCFS. The observed fluctuation spectra are broadband (40–300 kHz) with  $\bar{k}\rho_s \leq 0.1$ , where  $\bar{k}$  is the wavenumber of the fluctuations and  $\rho_s$  is the ion Larmor radius at the sound speed. The propagation direction of the fluctuations reverses to the electron diamagnetic direction around  $r/a < 1$ . The phase velocity and the electron drift velocity are comparable ( $v_{ph} \sim v_{de}$ ). The fluctuation-induced particle flux is comparable to fluxes estimated from the particle balance using the  $H_\alpha$  spectroscopic measurements. Many of the features seen in these experiments resemble the features of ohmically heated plasmas in the Texas Experimental Tokamak (TEXT).

\*Research sponsored by the Office of Fusion Energy, U.S. Department of Energy, under contract DE-AC05-84OR21400 with Martin Marietta Energy Systems, Inc., and DE-FG05-89ER53295 with the University of Texas at Austin.

\*\*Permanent address: Asociación EURATOM/CIEMAT, Madrid, Spain.

## **DISCLAIMER**

This report was prepared as an account of work sponsored by an agency of the United States Government. Neither the United States Government nor any agency thereof, nor any of their employees, makes any warranty, express or implied, or assumes any legal liability or responsibility for the accuracy, completeness, or usefulness of any information, apparatus, product, or process disclosed, or represents that its use would not infringe privately owned rights. Reference herein to any specific commercial product, process, or service by trade name, trademark, manufacturer, or otherwise does not necessarily constitute or imply its endorsement, recommendation, or favoring by the United States Government or any agency thereof. The views and opinions of authors expressed herein do not necessarily state or reflect those of the United States Government or any agency thereof.

## 1. Introduction

Energy and particle confinement in tokamaks and stellarators is anomalous, and results from the two types of devices show similar dependences on plasma parameters [1]. The study of electrostatic fluctuations [2] in different magnetic configurations may help to identify the underlying physics mechanisms responsible for plasma transport. To investigate the effects of the magnetic configuration on the characteristics of edge turbulence, recent measurements of electrostatic fluctuations at the edge of the Texas Experimental Tokamak (TEXT) [3] have been extended to the Advanced Toroidal Facility (ATF) [4] torsatron. Experimental observations on TEXT indicate that electrostatic fluctuations are the dominant mechanism for energy and particle losses in the edge [3,5]. To understand the driving forces on the edge turbulence in terms of the plasma current and the magnetic configuration, initial edge fluctuation measurements have been carried out on the currentless ATF device with a diagnostic setup similar to that used in the TEXT experiments, that is, a fast reciprocating Langmuir probe (FRLP) array [6].

The FRLP has been used to characterize, from an experimental point of view, the electrostatic turbulence on the edge of the ATF torsatron. The experimental setup and the analysis method are described in section 2. Measurements of plasma electron density  $n_e$ , electron temperature  $T_e$ , and fluctuations in density ( $\bar{n}_e$ ) and plasma floating potential ( $\tilde{\phi}_f$ ) at the edge of electron cyclotron heated (ECH) plasmas in ATF are presented and their turbulence characteristics are discussed in section 3. Brief conclusions follow in section 4.

## 2. Experimental setup

The stellarator configuration of the ATF torsatron has a poloidal multipolarity  $\ell = 2, 12$  field periods ( $M = 12$ ), a major radius  $R_0 = 2.1$  m, and an average plasma radius  $\bar{a} = 0.27$  m. The externally produced currentless magnetic configuration has moderate shear; that is, the central rotational transform ( $1/2\pi = 1/q$ ) of 0.3 becomes 1.0 at the last closed flux surface (LCFS). Initial fluctuation measurements in ATF were carried out around the LCFS with the FRLP in ECH plasmas at a magnetic field  $B = 1$  T. Plasmas were created using a gyrotron source at 53 GHz with heating power  $P = 200$  kW. In these ECH plasmas, a representative range for the line-averaged plasma density is  $\bar{n}_e = (3-6) \times 10^{12}$  cm $^{-3}$ , and the plasma stored energy  $W_p \approx 1-2$  kJ.

The FRLP is located one field period away from the instrumented rail limiter [7]. The probe is inserted into the edge plasma from the top, moves 5 cm into the plasma in 50 ms, and remains there about for 40 ms to carry out the fluctuation measurements. The FRLP head consists of a square array of four tips, 0.5 mm in diameter, that are 2 mm long and 2 mm apart. Double Langmuir probe operation of two tips, aligned perpendicular to the local magnetic field, makes it possible to measure the edge plasma  $n_e$ ,  $T_e$ , and  $\bar{n}_e/n_e$  profiles inside (about 2 cm) and outside the LCFS, as indicated in fig. 1. The other two tips are used to measure  $\tilde{\phi}_f$  and the wavenumber  $k$  perpendicular to the local magnetic field. The data have been analysed using spectral analysis techniques [8]. That is, the fluctuation signals are digitized at 1 MHz, and fast Fourier transform (FFT) is used to obtain their power spectrum  $S(k, \omega)$  as a function of frequency  $\omega$  and  $k$  using the two-probe technique described in ref. [9]. Ensemble averaging of the spectral distribution of the flux  $\tilde{\Gamma}(\omega)$ , obtained from the correlation of density and plasma potential fluctuations ( $\tilde{\phi}_p$ ), gives the turbulence-induced radial particle flux:

$$\tilde{\Gamma} = \langle \tilde{n}_e \tilde{v}_r \rangle = 2 \sum_{\omega > 0} \tilde{\Gamma}(\omega). \quad (1)$$

Here  $\tilde{v}_r = -ik\tilde{\phi}_p/B$  is the radial velocity due to the electrostatic fluctuations, and the frequency-resolved flux is estimated from many independent realizations using a triple correlation technique [10]:

$$\tilde{\Gamma}(\omega) = \text{Re}[\langle -ik(\omega)\tilde{n}_e^*(\omega)\tilde{\phi}_p(\omega) \rangle]/B. \quad (2)$$

Further, to gain an insight into the physical process,  $\tilde{\Gamma}(\omega)$  can be expressed as [8]

$$\tilde{\Gamma}(\omega) \approx (k/B)\gamma_{\tilde{n}\tilde{\phi}} n_{\text{rms}} \phi_{\text{rms}} \sin \theta_{\tilde{n}\tilde{\phi}}, \quad (3)$$

where  $\gamma_{\tilde{n}\tilde{\phi}}$  is the coherence,  $\theta_{\tilde{n}\tilde{\phi}}$  is the phase angle between the density and potential fluctuations, and  $n_{\text{rms}}$  and  $\phi_{\text{rms}}$  are the rms values of the fluctuations.

### 3. Results and discussion

Spatial profiles of the edge plasma density and temperature and the plasma floating potential  $\phi_f$  are shown in fig. 2 for  $0.95 < r/a < 1.15$ . These measurements were made during the steady-state phase of the plasma discharge. The plasma potential  $\phi_p$  may be estimated from the measurements of  $\phi_f$  and  $T_e$  as  $\phi_p \approx \phi_f + \delta_p T_e$ , where  $\delta_p$  depends on the probe material, the heat load on the probe, the ion species and its temperature, and the secondary electron emission coefficient. Typically,  $\delta_p \sim 1-3$  for hydrogen plasmas [11]. Around the LCFS,  $r/a \approx 1$ , the plasma parameters are  $n_e = (1-1.2) \times 10^{12} \text{ cm}^{-3}$  and  $T_e = 30-40 \text{ eV}$ . The characteristic density and temperature scale lengths are  $L_n = [-(1/n_e)(dn_e/dr)]^{-1} \approx 3-4 \text{ cm}$  and  $L_T = 2L_n$ , respectively. These values are comparable (within a factor of 2) to those for ohmically heated plasmas in TEXT at 2 T [3].

Typical values for the normalized density ( $\tilde{n}_e/n_e$ ) and potential ( $\tilde{\phi}_f/T_e$ ) fluctuations (see fig. 3 for profiles) around the LCFS are  $\tilde{n}_e/n_e \approx 0.05-0.1$  and  $\tilde{\phi}_f/T_e \approx 0.1-0.2$ , which are lower than those in TEXT plasmas [3]. Although the correlation between  $\tilde{\phi}_f$  and temperature fluctuations  $\tilde{T}_e$  in ATF is not yet known, the contribution of  $\tilde{T}_e$  to  $\tilde{\phi}_f$  has been neglected because the measured values of  $\tilde{T}_e$  on TEXT were relatively small ( $\tilde{T}_e/T_e \approx 0.4\tilde{n}_e/n_e$ ) [12]. Fluctuation levels decrease as the probe is moved into the core plasma, where  $T_e > 20 \text{ eV}$  and  $\tilde{\phi}_f/T_e \approx 2\tilde{n}_e/n_e$  at  $r/a = 0.95$ .

Fluctuation spectra of  $\tilde{n}_e$  and  $\tilde{\phi}_f$  have been examined for frequencies up to 400 kHz. Observed wavenumber-frequency power spectra  $S(k, \omega)$  are broadband and mostly in the range 40–300 kHz (as seen in figs. 4 and 5). The estimated mean value of the wavenumbers from the two probe measurements is  $\bar{k} = 1-3 \text{ cm}^{-1}$ , which satisfies  $\bar{k}\rho_s = 0.05-0.1$ , where  $\rho_s$  is the ion Larmor radius at the sound speed, as observed in TEXT [3]. Analysis of the wavenumber spectra shows that inside the LCFS the spectral width  $\sigma_k$ , the rms deviation about  $\bar{k}$ , decreases with increasing local electron temperature (fig. 6), indicating that the correlation length  $L_c = 1/\sigma_k$  increases with temperature [13] and typically  $L_c \approx 1 \text{ cm}$ , which is much larger than the probe tip separation, for  $T_e > 35 \text{ eV}$ . The integrated potential fluctuation power spectra  $S(\omega)$  and  $S(k)$  decrease for large  $\omega$  ( $> 200 \text{ kHz}$ ) and  $k$  (as illustrated in fig. 5) with dependences given by  $S(\omega) \sim \omega^{-\alpha}$  and  $S(k) \sim k^{-\beta}$ , where  $\alpha \sim \beta \approx 4 \pm 1$ . The shape of the  $\tilde{n}$  spectrum is generally similar to that of  $\tilde{\phi}_f$ .

The fluctuation-induced particle flux is estimated from eqs. (1) and (2) by taking  $\tilde{\phi}_p \approx \tilde{\phi}_f$ . The coherence between the density and the floating potential fluctuations is  $\gamma_{\tilde{n}\tilde{\phi}} \approx 0.8$  up to 150 kHz, dropping to  $\sim 0.2$  beyond 250 kHz, and the corresponding phase angle is  $\theta_{\tilde{n}\tilde{\phi}} \approx 70^\circ$  around 150 kHz. The frequency-resolved particle flux  $\tilde{\Gamma}(\omega)$  is dominated by frequencies below 250 kHz

(fig. 7) and reaches a maximum at 100–150 kHz, where the phase angle has its maximum. The spatial profile of the total particle flux  $\tilde{\Gamma}$ , eq. (1), is given in fig. 8 for two representative line-averaged densities  $\bar{n}_e = 3.5 \times 10^{12} \text{ cm}^{-3}$  and  $5.5 \times 10^{12} \text{ cm}^{-3}$ . The radial flux is always outward and at the LCFS has a value  $\tilde{\Gamma} \sim 3 \times 10^{15} \text{ cm}^{-2} \cdot \text{s}^{-1}$  for  $\bar{n}_e = 3.5 \times 10^{12} \text{ cm}^{-3}$  and  $1.2 \times 10^{15} \text{ cm}^{-2} \cdot \text{s}^{-1}$  for  $\bar{n}_e = 5.5 \times 10^{12} \text{ cm}^{-3}$ . For the nearly flat core density profiles observed in ATF, the corresponding fluctuation-induced particle confinement times, assuming that  $\tilde{\Gamma}$  is constant on flux surfaces, are  $\tau_p = (\bar{a}/2)\bar{n}_e/\tilde{\Gamma} \sim 16 \text{ ms}$  and  $60 \text{ ms}$ , respectively. The associated local density diffusion coefficient is  $D_n = \tilde{\Gamma}L_n/n_e \sim 1 \times 10^4 \text{ cm}^2 \cdot \text{s}^{-1}$ , where  $n_e(\text{edge}) \sim 10^{12} \text{ cm}^{-3}$  and  $L_n \sim 4 \text{ cm}$  for both  $\bar{n}_e$  cases. Although detailed scans of  $\bar{n}_e$  have not yet been carried out in ATF to determine the scaling of  $\tilde{\Gamma}$  with  $\bar{n}_e$ , results from the present limited scans indicate that  $\tau_p$  increases with  $\bar{n}_e$  in these low-density regime studies. This observation is consistent with the TEXT results [14]. In ATF, it is rather difficult to use  $H_\alpha$  spectroscopic measurements for estimating the particle fluxes at the edge because of the lack of a full set of spectroscopic monitors to cover the complicated edge geometry and the existence of particle sources from the divertor stripes around the LCFS [15]. Nonetheless, some comparisons can be made. Based on available data from  $H_\alpha$  measurements, the estimated particle flux from the particle balance is  $\Gamma_{H_\alpha} \sim (1-1.5) \times 10^{15} \text{ cm}^{-2} \cdot \text{s}^{-1}$  for  $\bar{n}_e = 5.5 \times 10^{12} \text{ cm}^{-3}$ , which is comparable to  $\tilde{\Gamma}$ . This suggests that the electrostatic edge turbulence may be responsible for particle confinement characteristics in ATF.

A spatial profile of the mean phase velocity of the fluctuations,  $v_{ph} = 2\sum_{\omega>0} v_{ph}(\omega)$  with  $v_{ph}(\omega) = \sum_k (\omega/k)S(k,\omega)/\sum_k S(k,\omega)$ , is given in fig. 9. As observed on TEXT [2], the propagation of the fluctuations is in the ion diamagnetic direction for  $r/\bar{a} > 1$ , but it reverses to the electron diamagnetic direction for  $r/\bar{a} < 1$ . The location of the  $v_{ph}$  shear layer nearly coincides with the peak of the plasma potential where the radial electric field  $E_r = -d\phi_p/dr$  changes its direction from outward to inward, as shown in fig. 10 for  $\delta_p \sim 2.5$ . At this location, the density and electron temperature gradients are nearly zero and  $v_{ph} \sim v_e \sim 0$ , where  $v_e = (T_e/eB)(1/L_n + 1/L_T) - E_r/B$  is the electron drift velocity. Also, well inside the LCFS, where  $E_r \approx 0$ , it is found that  $v_{de} \approx v_{ph} \approx 10^3 \text{ m/s}$ .

Future experiments will include measuring the electron temperature fluctuations using the techniques given in refs. [12,16] to determine the relationship between  $\tilde{\phi}_p/T_e$  and  $\bar{n}_e/n_e$ , scaling of the edge fluctuation parameters with  $\bar{n}_e$ , and extending the experiments to ECH plasmas with  $B = 2 \text{ T}$  and neutral-beam-heated plasmas. The heavy ion beam probe diagnostic [17] should provide additional information on the plasma potential and its fluctuations.

#### 4. Conclusion

The initial results indicate substantial similarities in the characteristics of edge turbulence in the ohmically heated TEXT tokamak and the currentless ATF torsatron. The fluctuation-induced particle flux is consistent with the total particle flux estimated from the global particle balance. Thus, electrostatic turbulence may be responsible for the edge particle transport. Detailed comparison of the ATF and TEXT results can serve as the basis for development of a unified physics interpretation of edge turbulence in toroidal devices.

#### Acknowledgements

The authors thank B. A. Carreras, J. N. Leboeuf, P. H. Diamond, and D. R. Thayer for valuable discussions, M. Murakami and the other members of the ATF group and operating staff for help in carrying out the experiments, and J. Sheffield for continual support and encouragement.

## References

- [1] S. Sudo et al., Nucl. Fusion 30 (1990) 11.
- [2] P. Liewer, Nucl. Fusion 15 (1975) 487.
- [3] Ch.P. Ritz, R.D. Bengtson, S.J. Levinson, and E.J. Powers, Phys. Fluids 27 (1984) 2956; Ch.P. Ritz et al., Nucl. Fusion 27 (1987) 1125.
- [4] J.F. Lyon et al., Fusion Technol. 10 (1986) 179.
- [5] Ch.P. Ritz et al., Phys. Rev. Lett. 62 (1989) 1844.
- [6] Ch. P. Ritz, to be published.
- [7] T. Uckan et al., Bull. Am. Phys. Soc. 33 (1988) 2069.
- [8] E.J. Powers, Nucl. Fusion 14 (1974) 749.
- [9] J.M. Beall, Y.C. Kim, and E.J. Powers, J. Appl. Phys. 43 (1982) 3993.
- [10] Ch.P. Ritz et al., Rev. Sci. Instrum. 59 (1988) 1739.
- [11] P.C. Stangeby, Plasma sheath, in: Physics of Plasma-Wall Interactions in Controlled Fusion, Eds. D.E. Post and R. Behrisch (Plenum, New York, 1986) p. 41.
- [12] H. Lin, R.D. Bengtson, and Ch.P. Ritz, Univ. of Texas, Report FRCR-334 (1989).
- [13] C. Hidalgo et al., to be presented at the 17th European Conference on Controlled Fusion and Plasma Physics, Amsterdam, The Netherlands, June 25–29, 1990.
- [14] W.L. Rowan et al., Nucl. Fusion 27 (1987) 1105.
- [15] P.K. Mioduszewski et al., in: Proc. 16th Eur. Conf. Controlled Fusion and Plasma Physics, Venice, 1989 (European Physical Society, 1989), Vol. 13B, p. 623.
- [16] D.C. Robinson and M. G. Rusbridge, Plasma Phys. 11 (1969) 73.
- [17] A. Carnevali et al., Rev. Sci. Instrum. 59 (1988) 1670.

## Figure Captions

Fig. 1. Constant flux surfaces and the location of the FRLP on ATF.

Fig. 2. Spatial profiles of the ATF edge plasma density, temperature, and floating potential.

Fig. 3. Relative fluctuation levels for edge density and potential.

Fig. 4. Wavenumber-frequency power spectrum for potential fluctuations.

Fig. 5. (a) Power spectrum of the potential fluctuations. (b) Wavenumber spectrum  $S(k)$ .

Fig. 6. Variations of  $\sigma_k$  with  $T_e$  inside the LCFS.

Fig. 7. Typical spectrum of the fluctuation-induced particle flux.

Fig. 8. Spatial profile of the fluctuation-induced particle flux at the edge.

Fig. 9. Spatial profile of the mean phase velocity  $v_{ph}$  of the fluctuations. Beyond the shear layer, the wave propagation is in the ion diamagnetic direction.

Fig. 10. Spatial profile of the estimated edge plasma potential  $\phi_p$ . The location of the  $v_{ph}$  shear layer nearly coincides with the peak of the plasma potential where the radial electric field  $E_r = -d\phi_p/dr$  changes its direction from outward to inward.

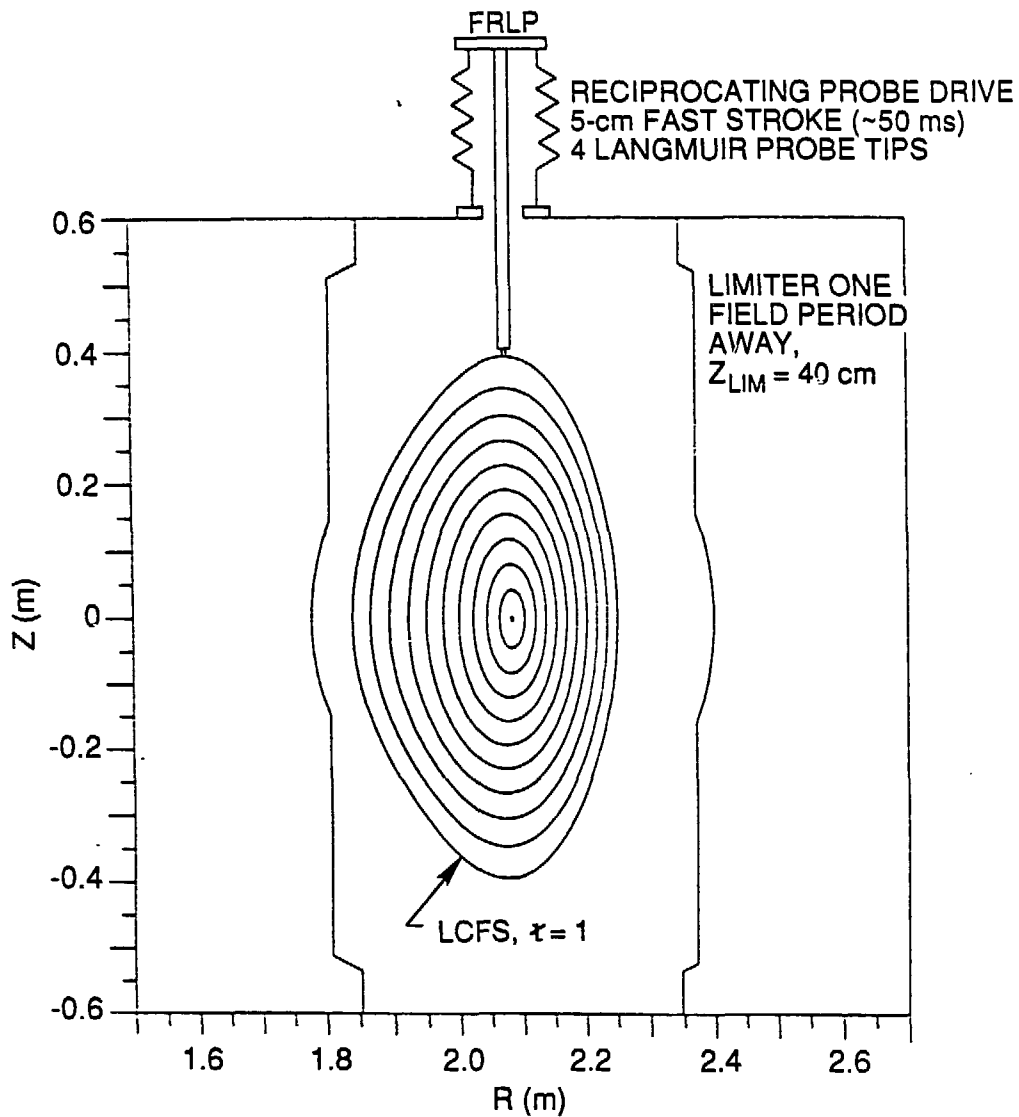


Fig. 1.

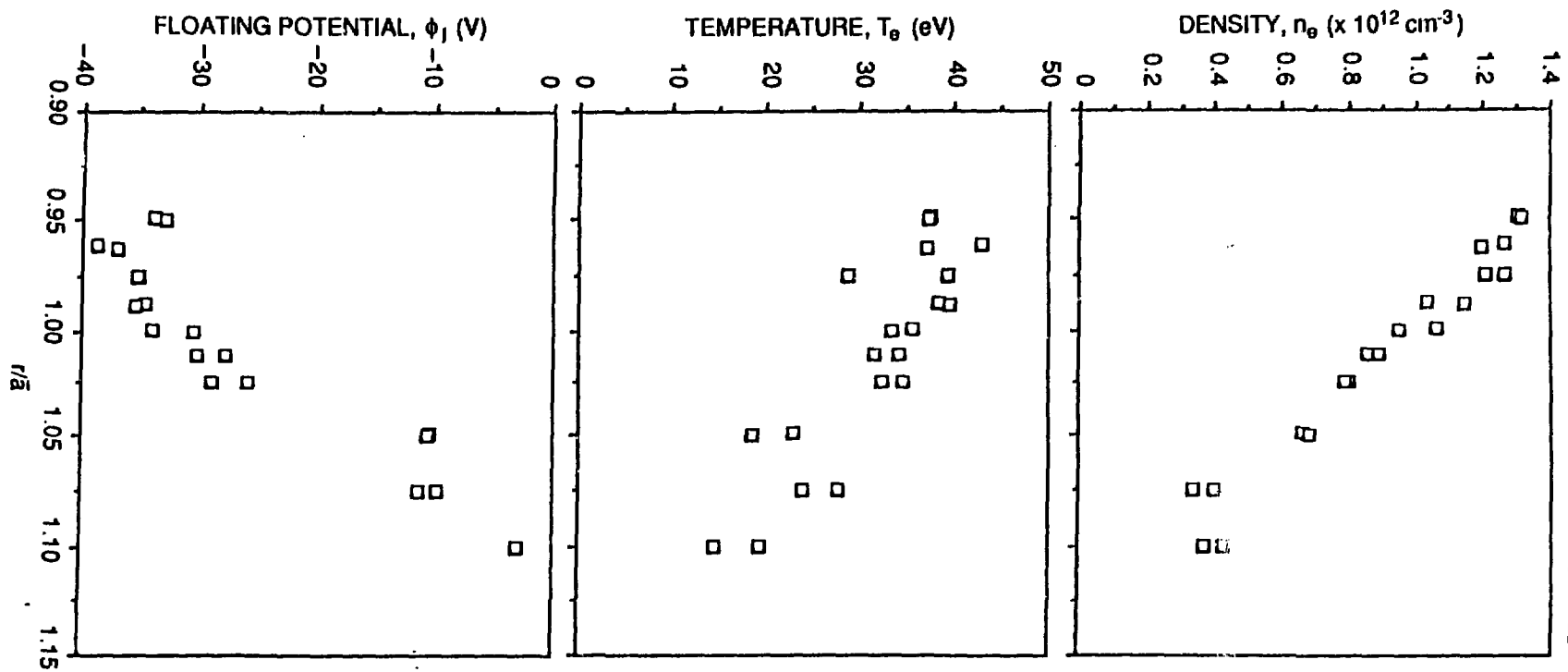


Fig. 2.

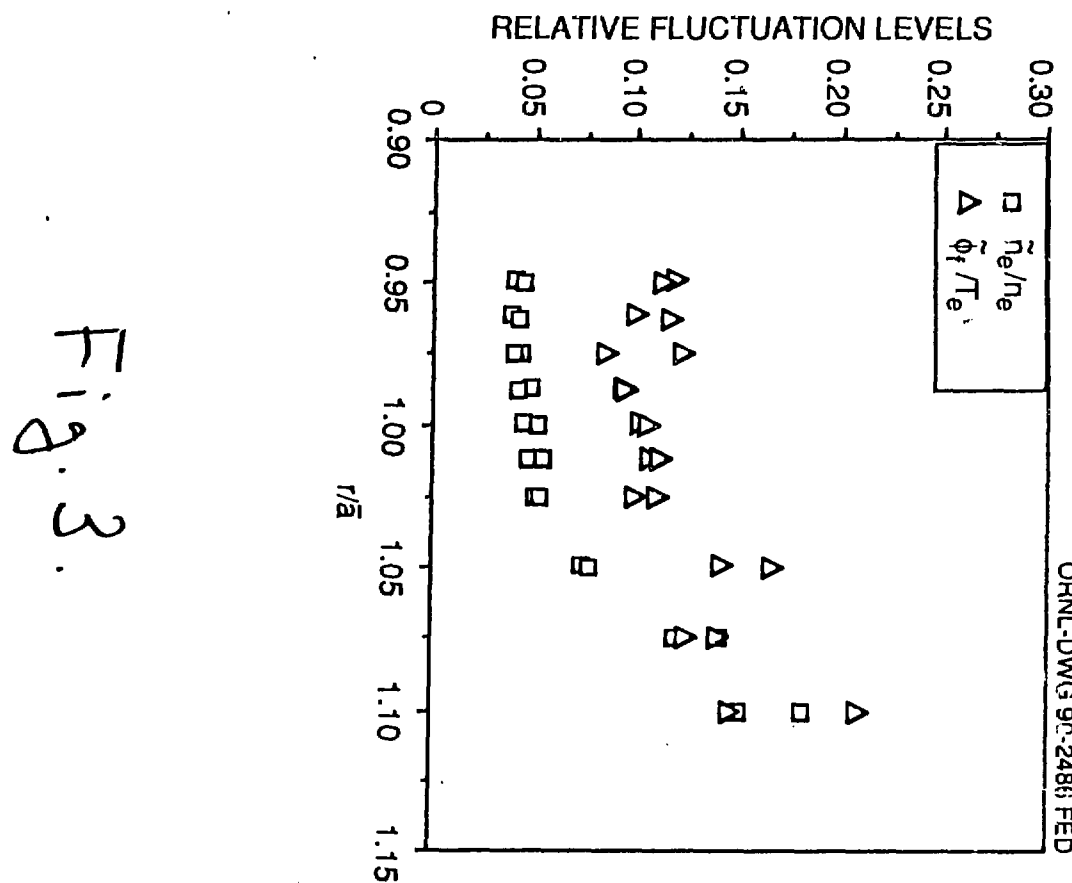


Fig. 3.

ORNL-DWG 90-2488 FED

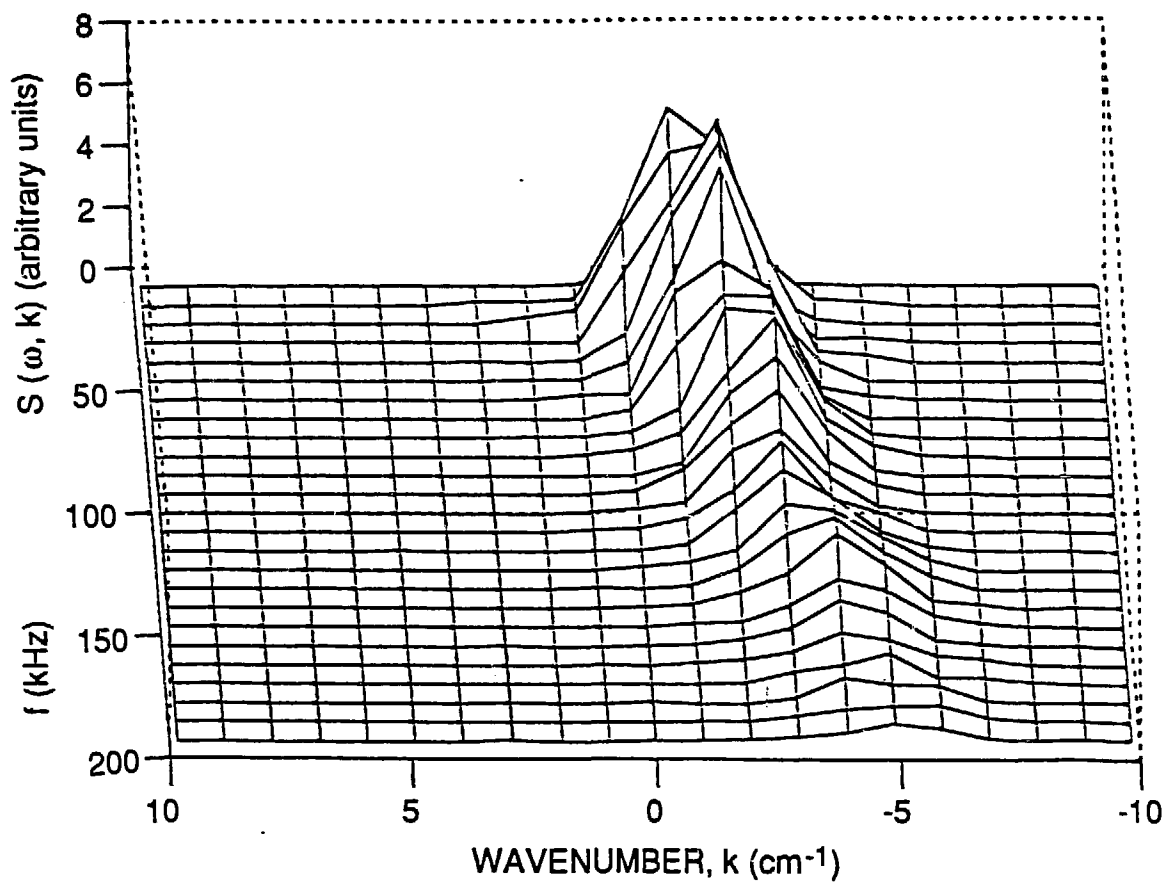


Fig. 4.

ORNL-DWG 90-2531 FED

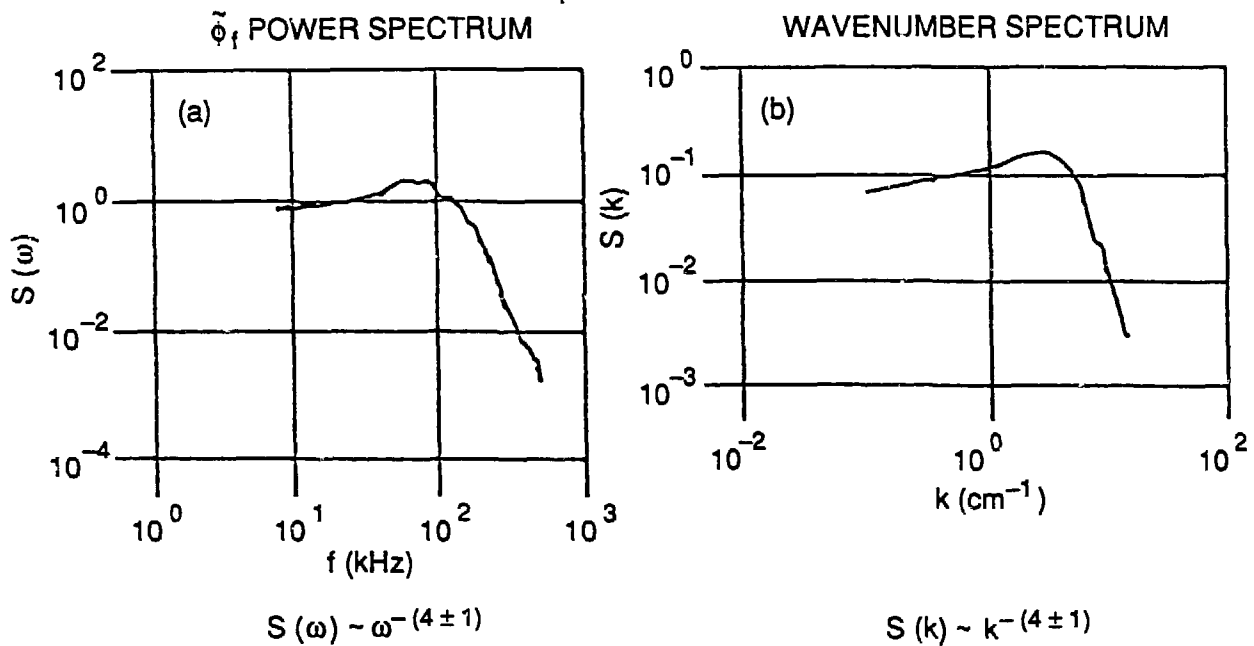


Fig. 5.

ORNL-DWG 90M-2533 FED

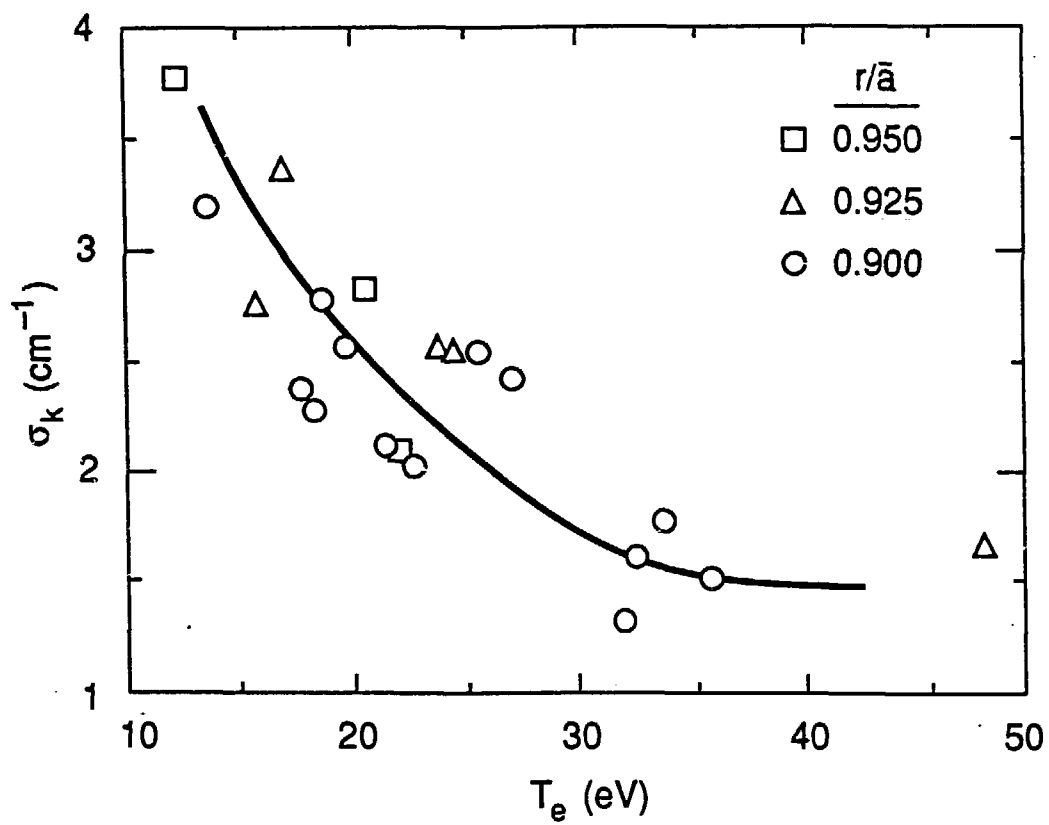


Fig. 6

ORNL-DWG 90-2489 FED

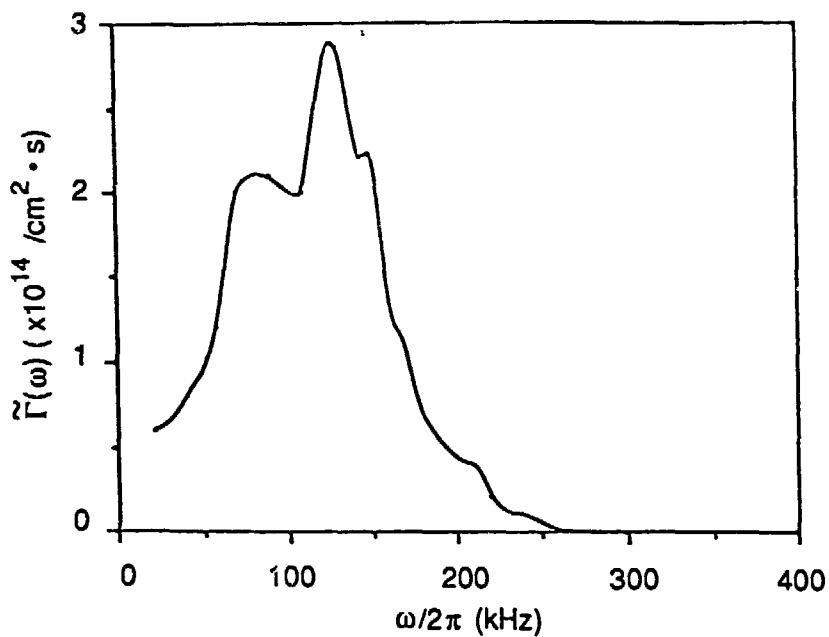


Fig. 7

ORNL-DWG 90M-2532 FED

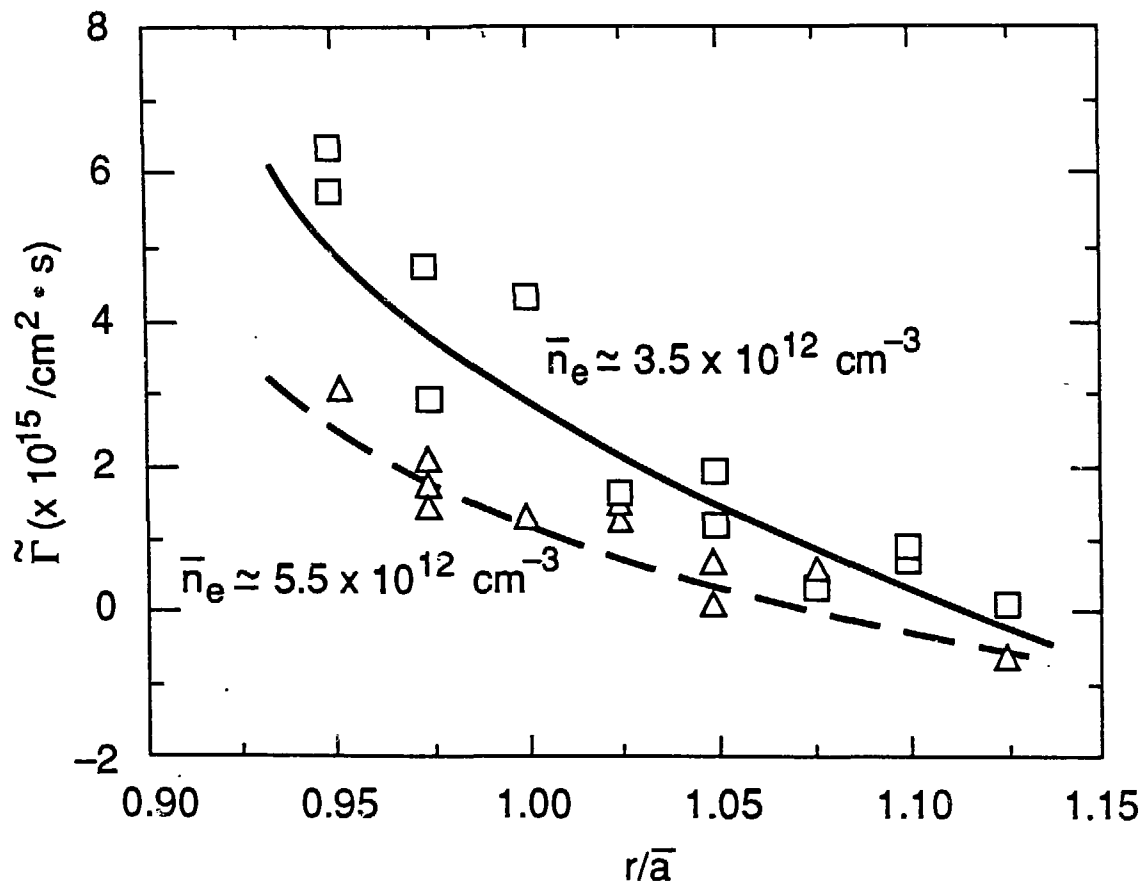
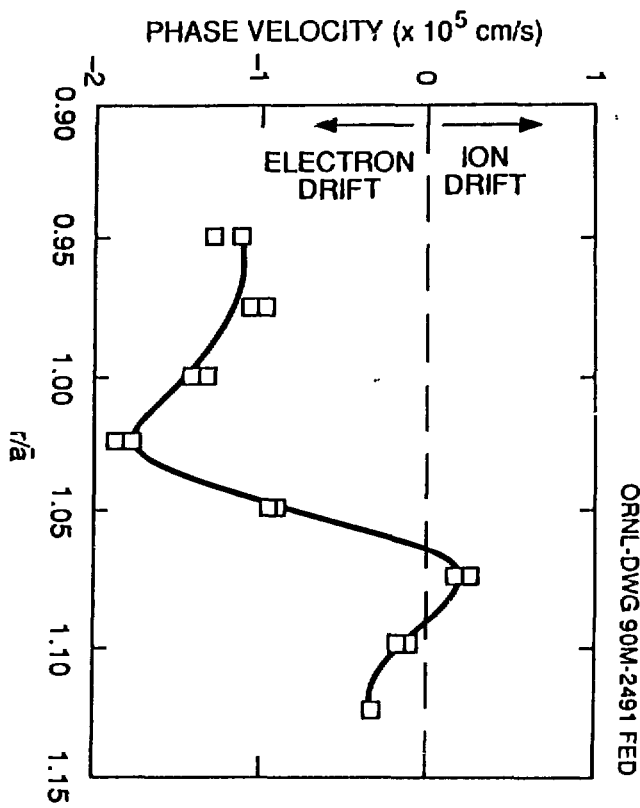


Fig. 8.

Fig. 9



ORNL-DWG 90-2492 FED

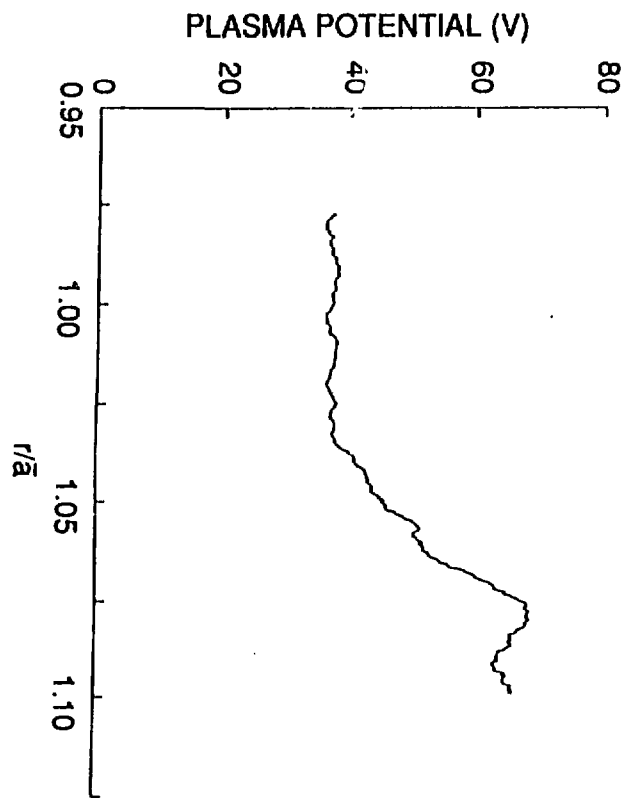


Fig. 10.

# ATF EDGE PLASMA TURBULENCE STUDIES USING A FAST RECIPROCATING LANGMUIR PROBE \*

T. Uckan, C. Hidalgo\*\*, J.D. Bell  
J.H. Harris, J.L. Dunlap, G. R. Dyer  
P.K. Mioduszewski, J.B. Wilgen

*Oak Ridge National Laboratory  
Oak Ridge, Tennessee, U.S.A.*

Ch. P. Ritz, A.J. Wootton, T.L. Rhodes, K. Carter

*Fusion Research Center, The Univ. of Texas  
Austin, Texas, U.S.A.*

*9th International Conference on Plasma Surface  
Interactions in Controlled Fusion Devices  
21-25 May 1990  
Bournemouth, UK*

---

\* Research sponsored by the Office of Fusion Energy, U.S. Department of Energy, under contract DE-AC05-84OR21400 with Martin Marietta Energy Systems, Inc., and under contract DE-FG05-89ER53295 with The University of Texas at Austin.

\*\* Permanent address: Asociación EURATOM/CIEMAT, Madrid, Spain.

MASTER

## **DISCLAIMER**

This report was prepared as an account of work sponsored by an agency of the United States Government. Neither the United States Government nor any agency thereof, nor any of their employees, makes any warranty, express or implied, or assumes any legal liability or responsibility for the accuracy, completeness, or usefulness of any information, apparatus, product, or process disclosed, or represents that its use would not infringe privately owned rights. Reference herein to any specific commercial product, process, or service by trade name, trademark, manufacturer, or otherwise does not necessarily constitute or imply its endorsement, recommendation, or favoring by the United States Government or any agency thereof. The views and opinions of authors expressed herein do not necessarily state or reflect those of the United States Government or any agency thereof.

## ABSTRACT\*

Experimental investigation of electrostatic turbulence on the edge of the ATF torsatron is carried out with a fast reciprocating Langmuir probe (FRLP) array. Initial measurements of plasma electron density  $n_e$  and temperature  $T_e$  and fluctuations in density ( $\tilde{n}_e$ ) and plasma floating potential ( $\tilde{\phi}_f$ ) are made in ECH plasmas at 1 T. At the last closed flux surface (LCFS,  $r/\bar{a} \sim 1$ ),  $T_e \approx 20-40$  eV and  $n_e \approx 10^{12}$  cm $^{-3}$  for a line-average electron density  $\bar{n}_e = (3-6) \times 10^{12}$  cm $^{-3}$ . Relative fluctuation levels, as the FRLP is moved into core plasma where  $T_e > 20$  eV, are  $\tilde{n}_e/n_e \approx 5\%$ , and  $e\tilde{\phi}_f/T_e \approx 2\tilde{n}_e/n_e$  about 2 cm inside the LCFS. Observed fluctuation spectra are broadband (40-300 kHz) with  $\bar{k}p_s \leq 0.1$ . Propagation of the fluctuations reverses to electron diamagnetic direction around  $r/\bar{a} < 1$ . The phase velocity and the electron diamagnetic drift velocity are comparable ( $v_{ph} \sim v_{de}$ ). Fluctuation-induced particle flux is comparable to those estimated from the particle balance using the H $\alpha$  spectroscopic measurements. Many of the features seen in these experiments resemble to those of ohmically heated plasmas in the TEXT tokamak.

---

\* Research sponsored by the Office of Fusion Energy, U.S. Department of Energy, under contract DE-AC05-84OR21400 with Martin Marietta Energy Systems, Inc., and under contract DE-FG05-89ER53295 with The University of Texas at Austin.

# Motivation, Purpose, and Summary

## Motivation:

- Experimental observations on TEXT indicate that the electrostatic fluctuations are the dominant mechanism for energy and particle losses in the edge [1,2].

## Purpose:

- Extend measurements of electrostatic fluctuations on the edge of TEXT to currentless ATF torsatron to investigate the effects of the magnetic configuration on the characteristics of the edge turbulence

⇒ **Characterize the electrostatic edge turbulence in ATF**

## Summary:

- Results from initial measurements indicate substantial similarities in characteristics of edge turbulence in ohmically heated TEXT tokamak and the currentless ATF torsatron.

# Tools and Outline

## Tools:

- Diagnostic setup: Similar to one in TEXT  
    ⇒ Fast reciprocating Langmuir probe (FRLP) array.
- Same statistical data analysis techniques are used between TEXT and ATF

## Outline:

- Experimental setup and analysis method
- Measurements of edge profiles of  $n_e$ ,  $T_e$ , plasma floating potential ( $\phi_f$ ) and relative fluctuation levels,  $(\tilde{n}_e/n_e)$  and  $(\tilde{\phi}_f/T_e)$ , in ECH plasmas
- Turbulence characteristics
- Observations on the particle balance and the shear layer
- Conclusions

# Experimental Set-up

- Initial fluctuation measurements in ATF were carried out around the LCFS ( $r/a \sim 1$ ) with the FRLP in ECH plasmas at  $B = 1$  T. (Measurements are made during the steady-state phase of the plasma discharge.)
- Double Langmuir probe operation of two tips, aligned  $\perp B$ ,  
measure  $\Rightarrow$  edge  $n_e$ ,  $T_e$ , and  $\tilde{n}_e/n_e$  profiles  
inside (about 2 cm) and outside LCFS  
-- see Fig. 1.
- Other two tips are floating,  
measure  $\Rightarrow \tilde{\phi}_f$  and  $k (\perp B)$

## Representative ATF Parameters

Major radius, $R_o$ (m)	2.1
Averaged plasma radius $\bar{a}$ (m)	0.27
Magnetic field, $B$ (T)	1.0
Multipolarity, $\ell$	2
Number of field periods, $\mathcal{M}$	12
Central rotational transform, $\iota(0)/2\pi$	0.3
Edge rotational transform, $\iota(\bar{a})/2\pi$	1.0
$P_{ECH}$ (@53 GHz) (kW)	200
$\bar{n}_e$ ( $10^{12} \text{ cm}^{-3}$ )	3-6
Plasma stored energy, $W_p$ (kJ)	1-2

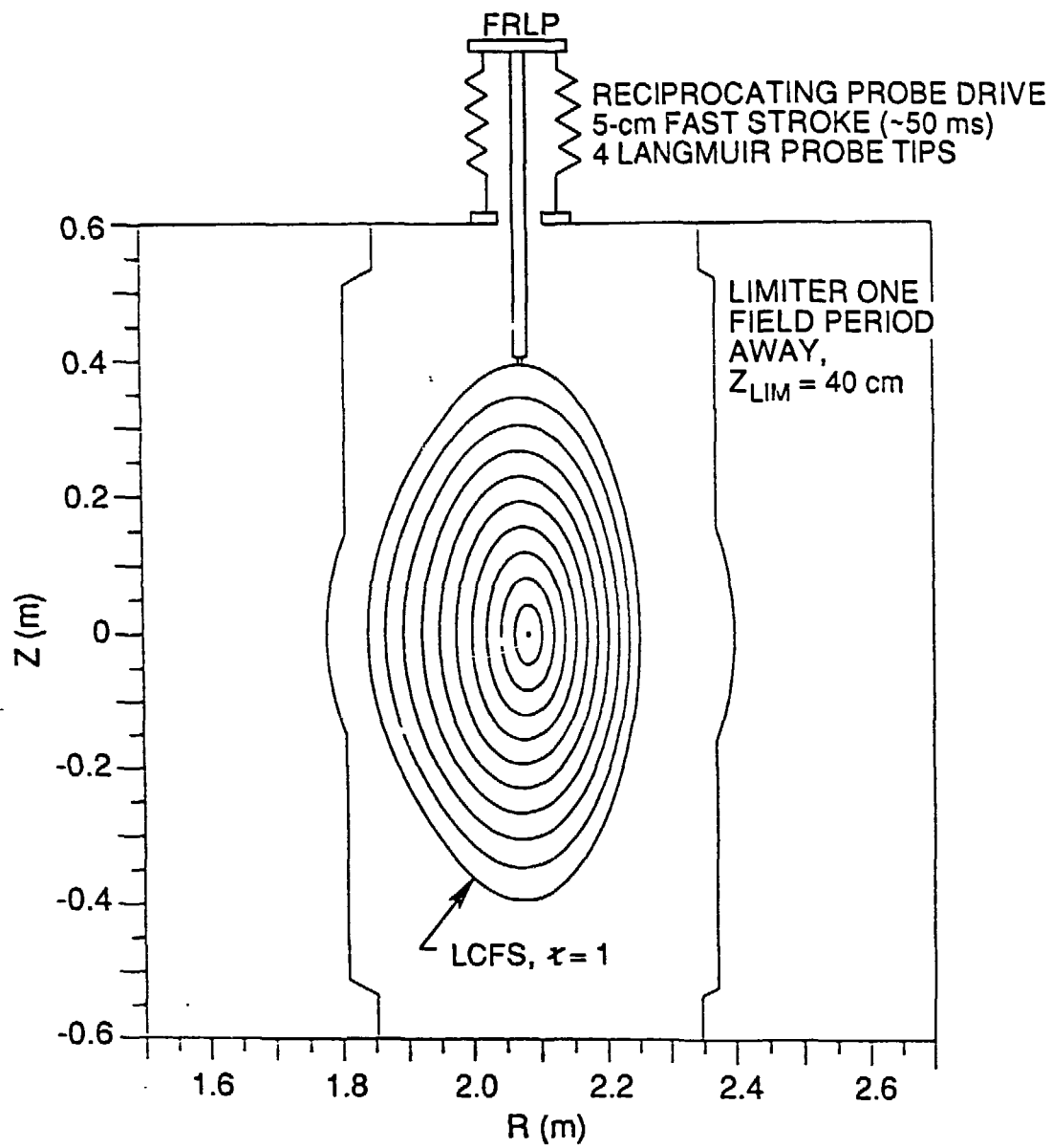


**Fig. 1** Flux surfaces and the location of the FRLP in ATF. FRLP head consists of a square array of four tips: 2 mm long and 2 mm apart. Probe moves 5 cm into the plasma in 50 ms, remains there  $\sim$ 40 ms.

## Data analysis:

- Data analysed using spectral analysis techniques [3].  
    ⇒ Fluctuation signals digitized at 1 MHz  
    ⇒ FFT used to obtain their power spectrum  $S(k, \omega)$  as a function of  $\omega$  and  $k$  using the two-probe technique [4].
- $\tilde{\Gamma}(\omega)$  obtained from the correlation of density and plasma potential fluctuations ( $\tilde{\phi}_p$ ), gives the turbulence-induced radial particle flux:

$$\tilde{\Gamma} = \langle \tilde{n}_e \tilde{v}_r \rangle = 2 \sum_{\omega > 0} \tilde{\Gamma}(\omega), \quad (1)$$

$\tilde{v}_r = -ik\tilde{\phi}_p/B$ , for the electrostatic fluctuations.

From the triple correlation technique [5] :

$$\tilde{\Gamma}(\omega) = \text{Re}[\langle -ik(\omega) \tilde{n}_e^*(\omega) \tilde{\phi}_p(\omega) \rangle]/B. \quad (2)$$

$$\approx (k/B) \gamma_{n\phi} n_{rms} \phi_{rms} \sin \theta_{n\phi}, \quad (3)$$

$\gamma_{n\phi}$  = coherence,  $\theta_{n\phi}$  = phase angle between  $\tilde{n}_e$  and  $\tilde{\phi}_p$  fluctuations,  $n_{rms}$  and  $\phi_{rms}$  = r.m.s. values of fluctuations.

# Results and Discussion

## Edge Plasma Properties

⇒ **Figure 2:** Spatial profiles of edge plasma  $n_e$ ,  $T_e$ , and floating potential  $\phi_f$  for  $0.95 < r/a < 1.15$ .

⇒ Plasma potential  $\phi_p$  can be estimated from

$\phi_p \approx \phi_f + \delta_p T_e$ , where  $\delta_p$  depends on probe material, heat load on the probe, the ion spice and its temperature, and the secondary electron emission coefficient. Typically,  $\delta_p \sim (1-3)$ .

[see **Fig. 10:**  $\phi_p$  is displayed for  $\delta_p \approx 2.5$ ]

⇒ Plasma parameters around LCFS,  $r/a \approx 1$ :

$n_e = (1-1.2) \times 10^{12} \text{ cm}^{-3}$  and  $T_e = (30-40) \text{ eV}$ .

⇒ Density and Temperature scale lengths:

$L_n = [-(1/n_e)(dn_e/dr)]^{-1} \approx (3-4) \text{ cm}$  and  $L_T \approx 2L_n$ .

These values are comparable (within a factor of 2) to those for ohmic plasmas in TEXT at 2 T.

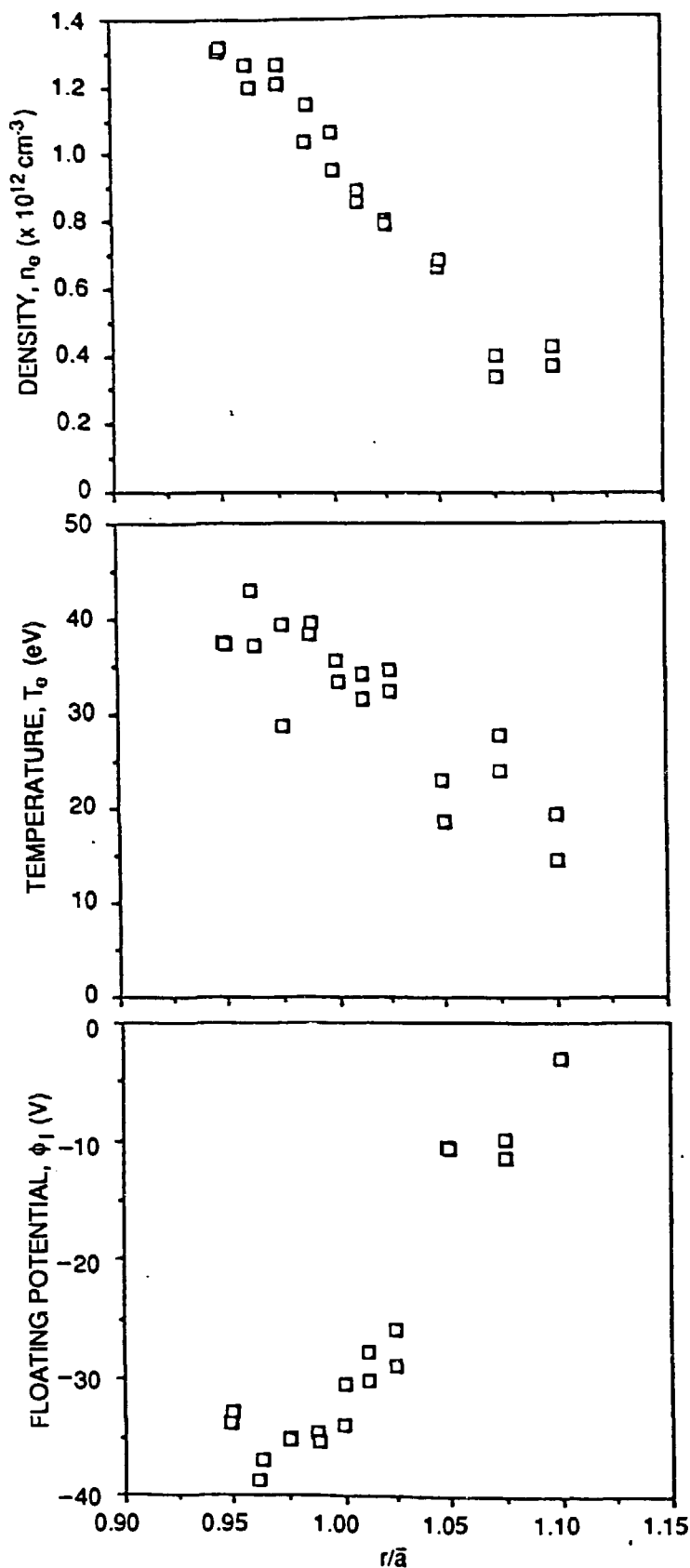


**Fig. 2** Spatial profiles of the ATF edge plasma density, temperature, and floating potential.

# Edge Fluctuations Characteristics

## Relative Fluctuation Levels

⇒ **Figure 3:** Spatial profiles of  $\tilde{n}_e/n_e$  and  $\tilde{\phi}_f/T_e$ .  
Typical values around the LCFS:  $\tilde{n}_e/n_e \approx (0.05-0.1)$  and  $\tilde{\phi}_f/T_e \approx (0.1-0.2)$ , lower than TEXT.  
⇒ Fluctuations decrease at  $r/\bar{a} \sim 0.95$ , where  $T_e > 20$  eV and  $\tilde{\phi}_f/T_e \approx 2\tilde{n}_e/n_e$ .

note In ATF correlation between  $\tilde{\phi}_f$  and  $\tilde{T}_e$  is not known, however, the contribution of  $\tilde{T}_e$  to  $\tilde{\phi}_p$  is neglected.  
recall: measured values of  $\tilde{T}_e$  on TEXT were relatively small ( $\tilde{T}_e/T_e \approx 0.4\tilde{n}_e/n_e$ ) [6].

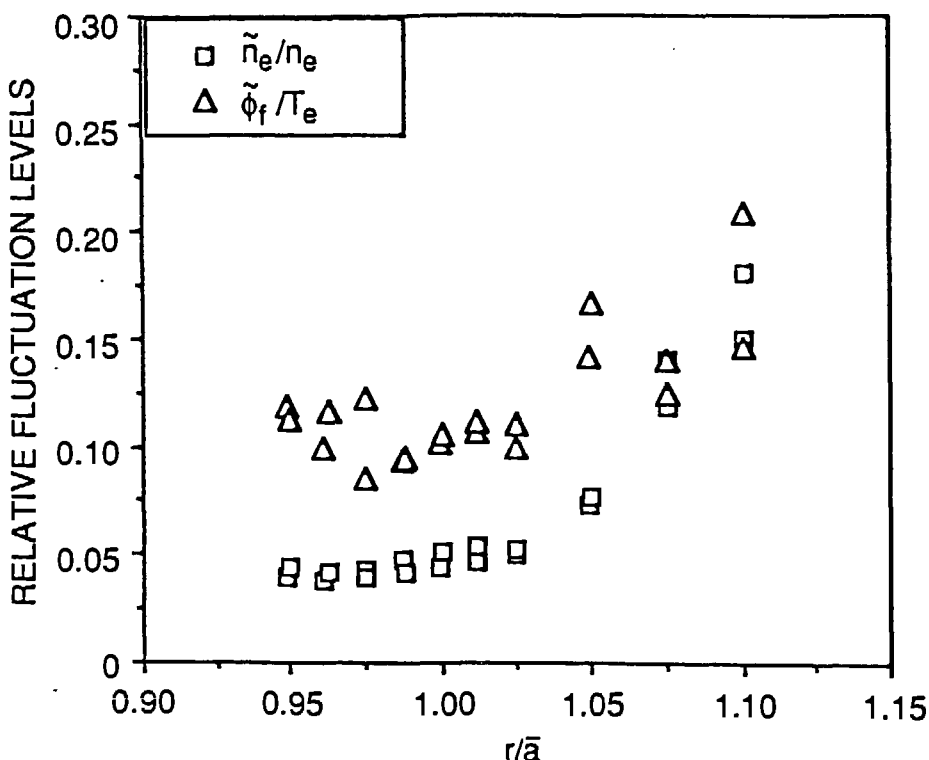


**Fig. 3** Relative fluctuation levels for edge density and plasma floating potential.

# Edge Fluctuations Characteristics (cont'd)

## Spectrum and Wavenumber

- ⇒ Fluctuation spectra examined up to 400 kHz.
- ⇒  $S(k, \omega)$  is broadband and mostly in 40–300 kHz range (see Figs. 4 and 5).
- ⇒ Estimated mean  $k$  value:  $\bar{k} = (1-3) \text{ cm}^{-1}$ , satisfies  $\bar{k}\rho_s \approx (0.05-0.1)$ , as observed in TEXT

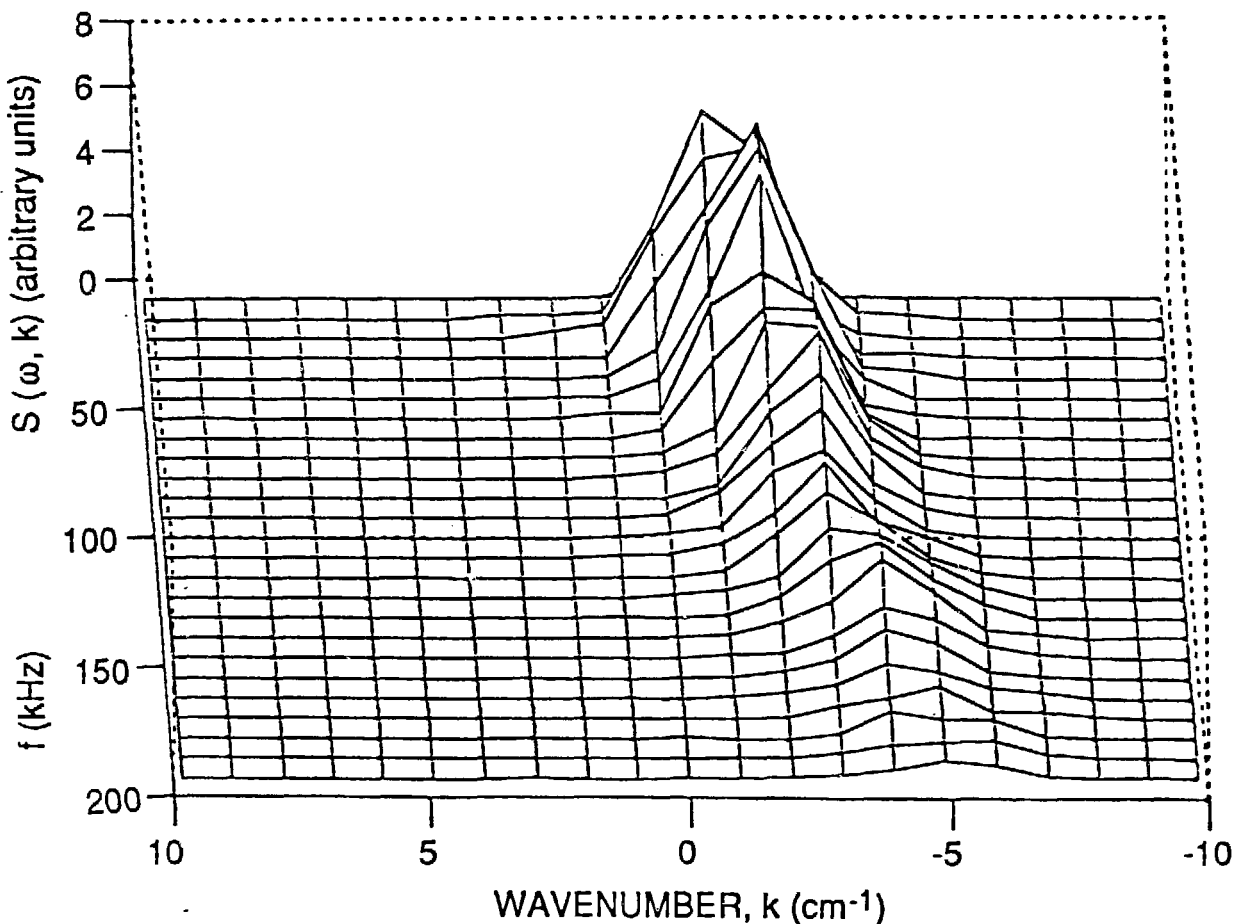


**Fig. 4** Wave number-frequency power spectrum for potential fluctuations.

# Edge Fluctuations Characteristics (cont'd)

## Spectrum and Wavenumber (cont'd)

⇒ **Figure 5:** Integrated  $\tilde{\phi}_f$  power spectra  $S(\omega)$  and  $S(k)$  decrease for large  $\omega$  ( $> 200$  kHz) and  $k$ :  
 $S(\omega) \sim \omega^{-\alpha}$  and  $S(k) \sim k^{-\beta}$ , with  $\alpha \sim \beta \approx 4 \pm 1$ .

⇒ Shape of  $\tilde{n}_e$  power spectrum is similar to  $\tilde{\phi}_f$ .

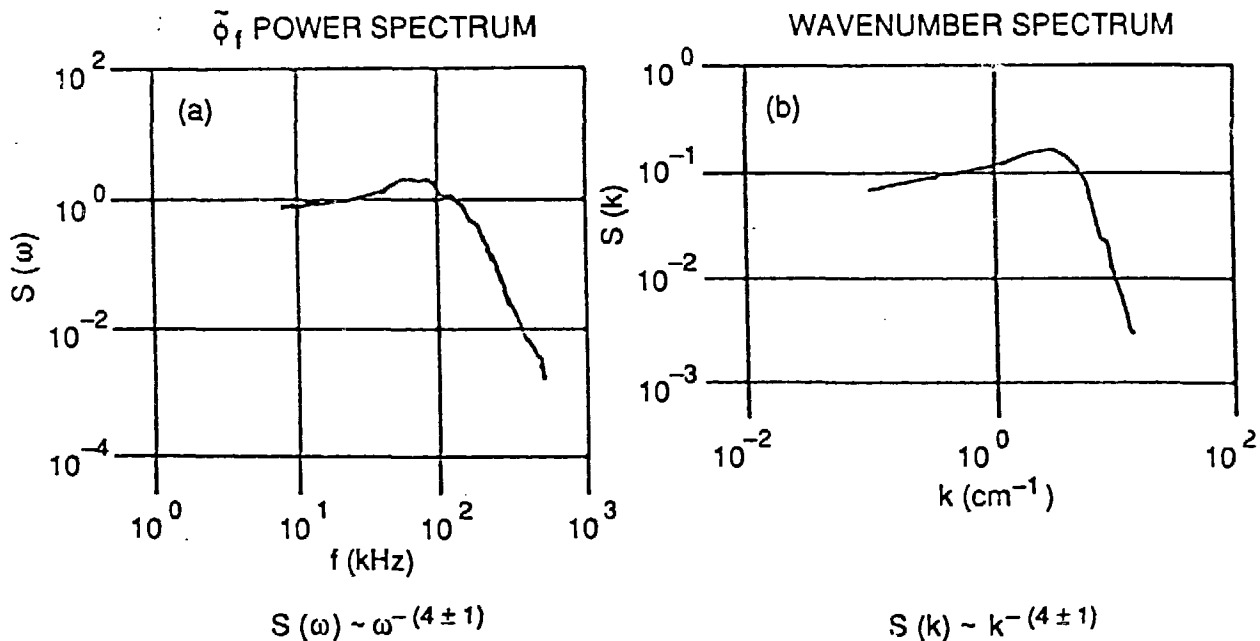


**Fig. 5** (a) Power spectrum of the potential fluctuations,  
(b) Wave number spectrum  $S(k)$ .

## Edge Fluctuations Characteristics (cont'd)

### Spectral Width

⇒ **Figure 6:** Inside LCFS, spectral width  $\sigma_k$  decreases with  $T_e$ , indicating correlation length  $L_c = 1/\sigma_k$  increases with  $T_e$  and  $L_c \approx 1$  cm for  $T_e > 35$  eV.

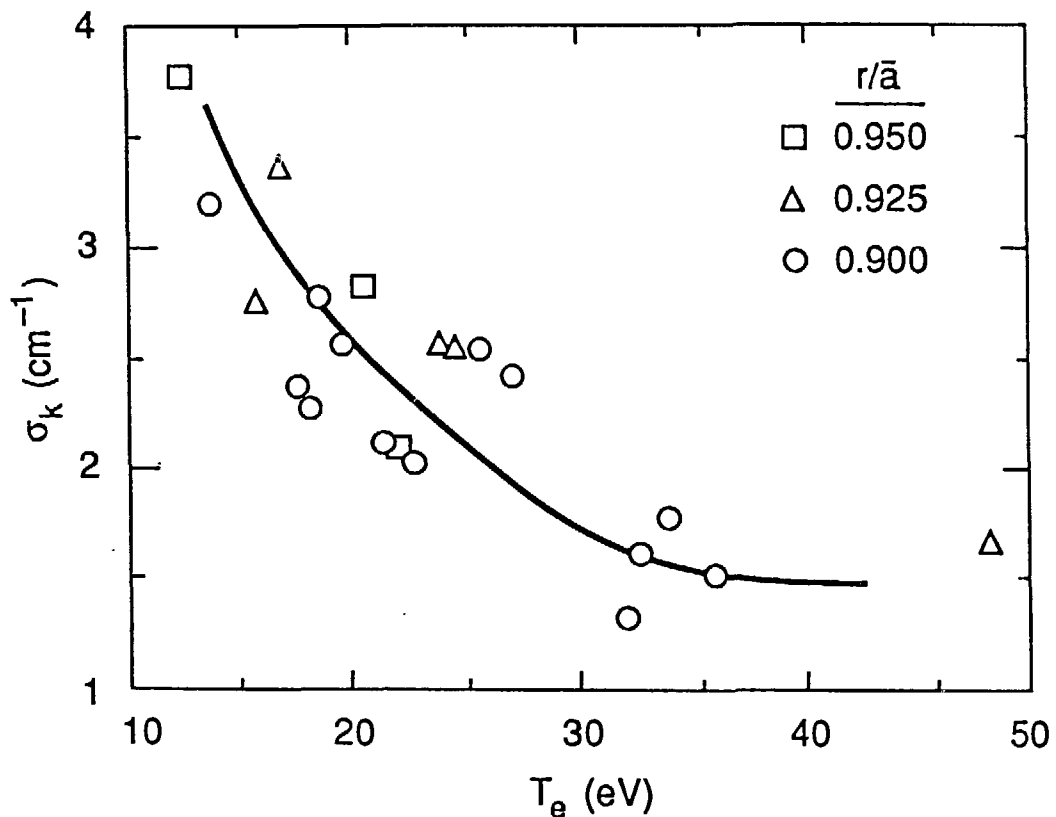


**Fig. 6** Variations of  $\sigma_k$  with  $T_e$  inside the LCFS.

# Edge Fluctuations Characteristics (cont'd)

## Fluctuation-induced Particle Fluxes

⇒ The fluctuation-induced total particle flux  $\tilde{\Gamma}$  is estimated from Eqs. (1) and (2) by taking  $\tilde{\phi}_p \approx \tilde{\phi}_f$ . The coherence is  $\gamma_{\tilde{\phi}} \approx 0.8$  up to 150 kHz, dropping to about 0.2 beyond 250 kHz.

The phase angle is  $\theta_{\tilde{\phi}} \approx 70^\circ$  around 150 kHz.

⇒  $\tilde{\Gamma}(\omega)$  dominated by below 250 kHz, (Fig. 7), and reaches a maximum at 100-150 kHz, where the phase angle has its maximum.

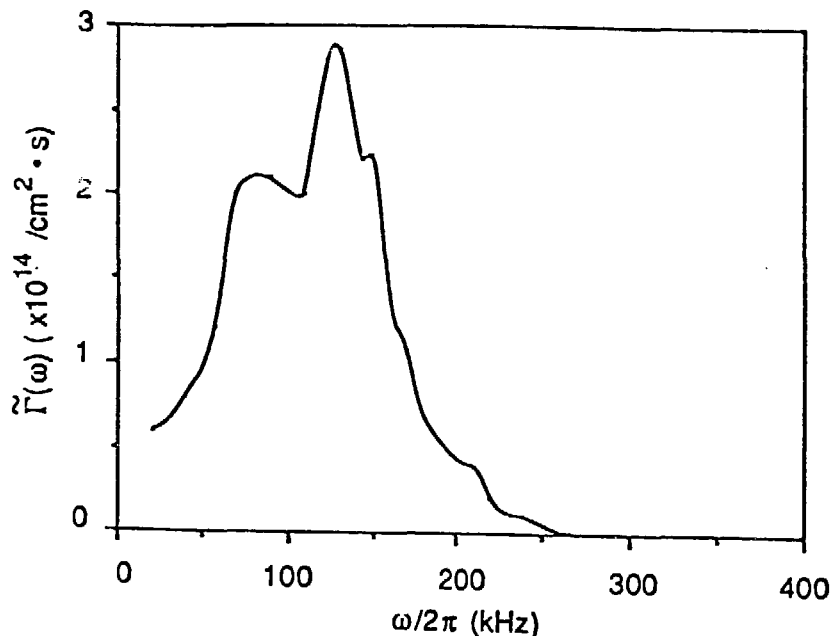


**Fig. 7** Typical spectrum of the fluctuations-induced particle flux.

# Edge Fluctuations Characteristics (cont'd)

## Fluctuation-induced Particle Fluxes (cont'd)

⇒ **Figure 8:**  $\tilde{\Gamma}$  profile for  $\bar{n}_e/10^{12} \text{ cm}^{-3} = 3.5$  and  $5.5$ . Radial flux is always outward and at the LCFS:  $\tilde{\Gamma} \sim 3 \times 10^{15} \text{ cm}^{-2 \cdot \text{s}^{-1}}$  for  $\bar{n}_e = 3.5 \times 10^{12} \text{ cm}^{-3}$  ( $\tilde{\Gamma} \sim 1.2 \times 10^{15} \text{ cm}^{-2 \cdot \text{s}^{-1}}$  for  $\bar{n}_e = 5.5 \times 10^{12} \text{ cm}^{-3}$ ).

⇒ For nearly flat core density profiles observed in ATF, the fluctuation-induced  $\tau_p$  is  $\tau_p = (\bar{a}/2)\bar{n}_e/\tilde{\Gamma} \sim 16 \text{ ms}$  and  $60 \text{ ms}$ , respectively.

⇒ Associated local density diffusion coefficient is  $D_n = \tilde{\Gamma}L_n/n_e \sim 10^4 \text{ cm}^2 \cdot \text{s}^{-1}$ ,  $n_e(\text{edge}) \sim 10^{12} \text{ cm}^{-3}$ ,  $L_n \sim 4 \text{ cm}$  for both  $\bar{n}_e$  cases.

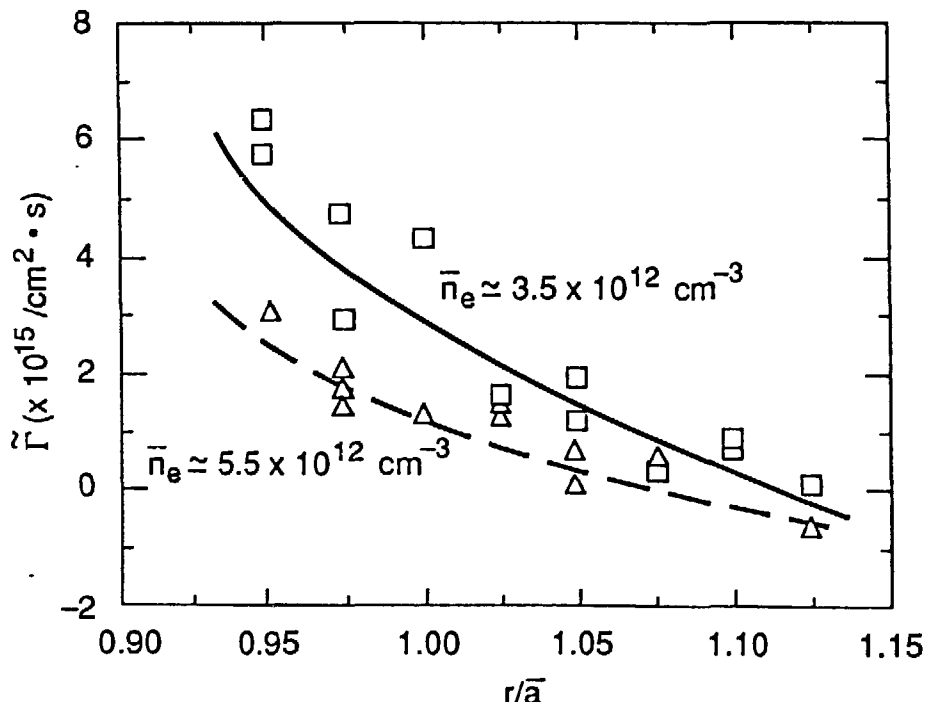


**Fig. 8** Profile of the fluctuations-induced particle flux

## Observations

### Particle Balance

- ⇒ Detailed  $\bar{n}_e$  scan experiments are not yet available. But, the limited scans indicate that  $\tilde{\tau}_p$  increases with  $\bar{n}_e$  in low density regime.
  - 👉 This observation is consistent with the TEXT results [7].
- ⇒ Particle flux from the particle balance using  $H_\alpha$  measurements is  $\Gamma_{H_\alpha} \sim (1-1.5) \times 10^{15} \text{ cm}^{-2}\text{s}^{-1}$  for  $\bar{n}_e = 5.5 \times 10^{12} \text{ cm}^{-3}$ ;
- ⇒  $\Gamma_{H_\alpha}$  comparable to  $\tilde{\Gamma}$ , suggesting that electrostatic edge turbulence may be responsible for particle confinement characteristics in ATF.

# Observations

## Shear Layer

⇒ **Figure 9:** Spatial profile of mean phase velocity of the fluctuations,  $v_{ph} = 2\sum_{\omega>0} v_{ph}(\omega)$ . As observed on TEXT, fluctuations propagate in ion diamagnetic direction for  $r/\bar{a} > 1$ , but it reverses to electron diamagnetic direction for  $r/\bar{a} < 1$ .

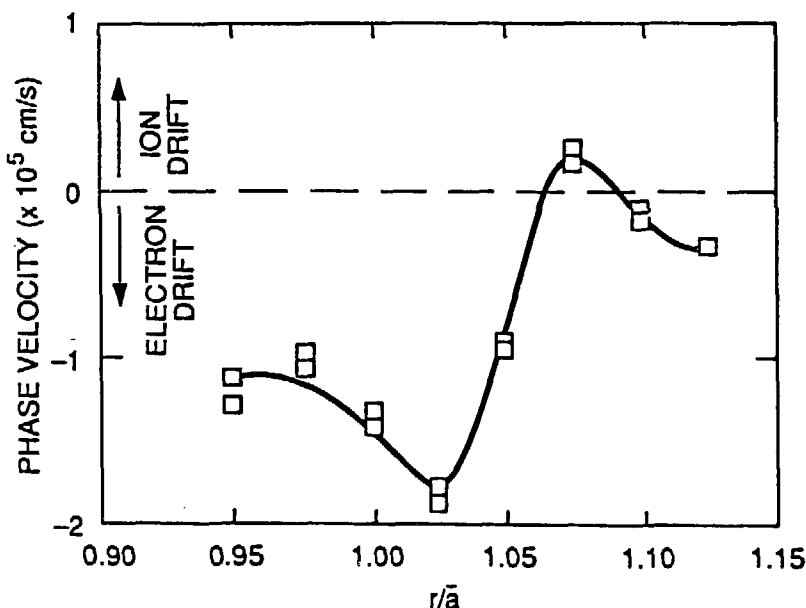


**Fig. 9** Spatial profile of  $\bar{v}_{ph}$  of fluctuations. Beyond the shear layer the wave propagation is in the ion diamagnetic direction.

## Observations (cont'd)

### Shear Layer

⇒ **Figure 10:** Location of  $v_{ph}$  shear layer coincides with peak of plasma potential, where  $E_r = -d\phi_p/dr$  changes direction from outward to inward

- At this location,  $\nabla n_e$  and  $\nabla T_e \sim 0$  and  $v_{ph} \sim v_{de} \sim 0$ , where  $v_{de} = (T_e/eB)(1/L_n + 1/L_T) - E_r/B =$  electron drift velocity.
- Well inside LCFS, where  $E_r \approx 0$ ,  $v_{de} \approx v_{ph} \approx 10^3$  m/s.

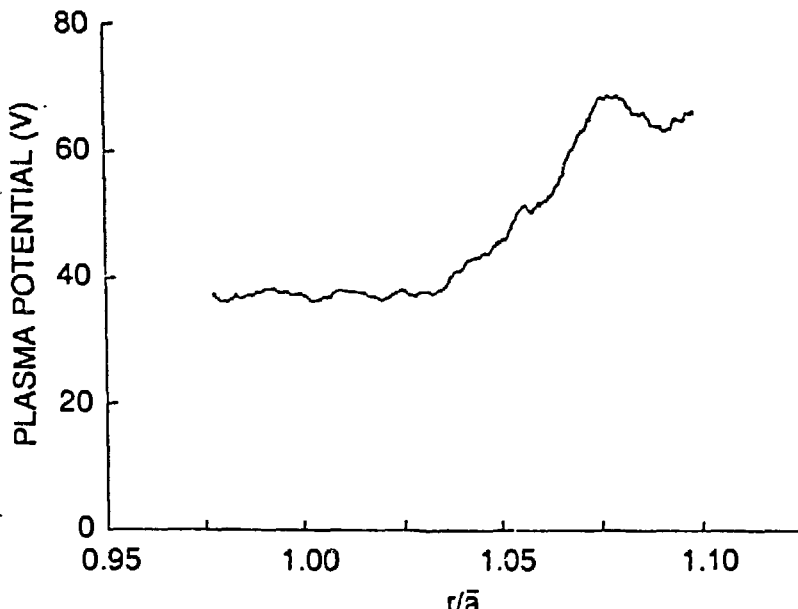


**Fig. 10** Plasma potential profile

## CONCLUSIONS

Results from initial measurements indicate substantial similarities in characteristics of edge turbulence in ohmically heated TEXT tokamak and the currentless ATF torsatron.

☞ Fluctuation characteristics are insensitive to plasma current.

Fluctuation-induced particle flux is consistent with the total particle flux estimated from the global particle balance (spectroscopic measurements).

☞ Electrostatic turbulence may be responsible for the edge particle transport.

Detailed comparisons of ATF and TEXT results can serve as basis for development of a unified physics interpretation of edge turbulence in toroidal devices.

## Future Plans

⇒ Future experiments will include

- measurement of  $T_e$  fluctuations [8] to determine relationship between  $\tilde{\phi}_p/T_e$  and  $\tilde{n}_e/n_e$ ,
- scaling of the edge fluctuation parameters with  $\bar{n}_e$ ,
- extension of experiments to ECH plasmas at 2 T,
- extension of experiments to neutral-beam-heated plasmas.

⇒ Additional information will be available from heavy ion beam probe diagnostic on plasma potential that will help to better characterize the edge turbulence on ATF.

## References

- [1] Ch. P. Ritz, R. D. Bengtson, S. J. Levinson, and E. J. Powers, Phys. Fluids **27**, (1984) 2956, and Ch. P. Ritz, et al., Nucl. Fusion **27** (1987) 1125.
- [2] Ch. P. Ritz, R. V. Bravenec, R. V. Schoch et al., Phys. Rev. Letters **62** (1989) 1844.
- [3] E. J. Powers, Nucl. Fusion **14**, (1974) 749.
- [4] J. M. Beall, Y. C. Kim, E.J. Powers, J. Appl. Phys. **43** (1982) 3933.
- [5] Ch.P.Ritz, E J. Powers, T. L. Rhodes, et al., Rev. Sci. Inst. **59**, (1988) 1739.
- [6] H. Lin, R. D. Bengtson, and Ch. P. Ritz, Univ. of Texas FRCR **334** (1989).
- [7] W. L. Rowan, et al., Nucl. Fusion **27** (1989) 1105.
- [8] D. C. Robinson and M. G. Rusbridge, Plasma Physics **11** (1969) 73.